DIRECTION-SELECTIVE ADAPTATION IN FLY VISUAL MOTION-SENSITIVE NEURONS IS GENERATED BY AN INTRINSIC CONDUCTANCE-BASED MECHANISM

R. KURTZ*

Department of Neurobiology, Bielefeld University, P.O. Box 100131, D-33501 Bielefeld, Germany

Abstract—Motion-sensitive neurons in the blowfly brain present an ideal model system to study the cellular mechanisms and functional significance of adaptation to visual motion. Various adaptation processes have been described, but it is still largely unknown which of these processes are generated in the motion-sensitive neurons themselves and which originate at more peripheral processing stages. By input resistance measurements I demonstrate that direction-selective adaptation is generated by an activity-dependent conductance increase in the motion-sensitive neurons. Based on correlations between dendritic Ca^{2+} accumulation and slow hyperpolarizing after-potentials following excitatory stimulation, a regulation of direction-selective adaptation by Ca^{2+} has previously been suggested. In the present study, however, adaptation phenomena are not evoked when the cytosolic Ca^{2+} concentration is elevated by ultraviolet photolysis of caged Ca^{2+} in single neurons rather than by motion stimulation. This result renders it unlikely, that adaptation in fly motion-sensitive neurons is regulated by bulk cytosolic Ca^{2+}. © 2007 IBRO. Published by Elsevier Ltd. All rights reserved.

Key words: after-hyperpolarization, blowfly, caged Ca^{2+}, Ca^{2+}-activated K^+-channels, input resistance, visual system.

Many sensory cells and neurons react to ongoing stimulation with a change in their response properties (reviews: Fain et al., 2001; Fettiplace and Ricci, 2003; Krekelberg et al., 2006). Such a dependency on stimulus history has been suggested to match neuronal sensitivity and filtering properties to the strength and the statistical properties of the current stimulus distribution (e.g. Dragoi et al., 2002; Benda et al., 2005). In the visual system, adaptation to moving stimuli has been shown to consist of different components, which can be classified according to their selectivity for pattern orientation. A large variety of adaptive properties was found in cat visual cortex V1 and V2, ranging from neurons that adapt to stimuli of any orientation to neurons that adapt only to optimally orientated

patterns (Sengpiel and Bonhoeffer, 2002; Crowder et al., 2006). Moreover, it has been reported that adaptation has the potential to shift the orientation tuning of individual neurons, leading to dynamic changes in the map of orientation preference in V1 (Dragoi et al., 2000).

In a group of individually identifiable visual motion-sensitive neurons in the blowfly (*Calliphora vicina*) brain called tangential cells (TCs), several components of motion adaptation have been described (Maddess and Laughlin, 1985; Harris et al., 2000; Brenner et al., 2000; Borst et al., 2005). Many TCs are amenable to electrophysiological and imaging techniques *in vivo* during presentation of sensory stimuli that are well-known to be behaviorally relevant (reviews: Borst and Haag, 2002; Egelhaaf et al., 2002, 2005). This has made fly vision an ideal model system to study both the mechanisms and the functional consequences of motion adaptation.

Most TCs spatially integrate on their retinotopically organized large dendrites the output signals of local motion-sensitive input elements. Thus, TCs respond to visual motion in a fully direction-selective way, being excited by motion in one direction and inhibited by motion in the opposite direction. Adaptation seems to operate on various levels of the motion-detection pathway through mechanisms located presynaptic to TCs, but possibly—although unproven so far—also in TCs themselves. This could be reflected in specific properties of the different components of motion adaptation: Contrast gain has been observed to be reduced by motion in any direction and may therefore originate from stages in the visual pathway prior to the computation of motion direction, i.e. upstream of TCs (Harris et al., 2000). Another component of adaptation only occurs during motion in the preferred direction (PD) of the TC and is associated with membrane after-hyperpolarization (AHP) when the stimulus terminates (Kurtz et al., 2000) and leads to a subtractive shift in the stimulus-response function (Harris et al., 2000). This form of direction-specific adaptation may either originate in TCs themselves or at a processing stage before TCs. The latter possibility would require the underlying mechanism to occur exclusively in elements providing TCs with excitatory inputs but not in those providing inhibitory inputs.

Prompted by correlations between dendritic Ca^{2+} accumulation and membrane AHP following excitatory stimulation, a Ca^{2+}-dependent inhibitory conductance, such as Ca^{2+}-activated K^+-channels, has been proposed as a physiological basis of direction-selective adaptation (Kurtz et al., 2000). Alternative to Ca^{2+}, Na^+ could also act as mediator of activity-dependent adaptation (review: Bhatta-

*Tel: +49-521-1065577; fax: +49-521-10689034.

E-mail address: rafael.kurtz@uni-bielefeld.de (R. Kurtz).

charjee and Kaczmarek, 2005). Although evidence for the involvement of Na^+ in adaptation is still scarce, Na^+-regulated adaptation in TCs remains distinctly possible, since voltage-clamp experiments and pharmacology suggest that Na^+-activated K^+-channels exist in TCs (Haag et al., 1997).

In the present study, I demonstrate that direction-specific adaptation is intrinsically generated in TCs by an activity-dependent mechanism. Furthermore, by directly manipulating cytosolic Ca^{2+} concentrations by ultraviolet (UV) photolysis of caged Ca^{2+} I show that direction-specific adaptation is probably not controlled by bulk cytosolic Ca^{2+}. Alternative explanations are the control of adaptation by a Na^+-regulated conductance, or by Ca^{2+}-regulated channels which co-localize with Ca^{2+} channels and which therefore temporarily experience much higher Ca^{2+} concentrations than during flash photolysis.

EXPERIMENTAL PROCEDURES

Preparation and electrophysiology

All experiments were carried out at room temperature (18–25 °C) on $\leq$3-day-old female blowflies, bred in the department's stock. After dissection as described in (Dürr and Egelhaaf, 1999) the fly was mounted under an upright fixed-stage microscope (Axioskop FS, Zeiss, Oberkochen, Germany) to view the fly brain from behind. Membrane potential recordings, Ca^{2+} imaging, and UV photolysis of caged Ca^{2+} were performed *in vivo* on TCs in the third visual neuropile of the fly, the lobula plate. Identification of individual TCs was based on their receptive field properties, specific characteristics of their electrical responses, and their anatomy, if visualized with fluorescent Ca^{2+} dyes.

Intracellular recordings from TCs were made using sharp borosilicate glass electrodes (GC100TF-10, Clark Electromedical, Edenbridge, UK) pulled on a Brown-Flaming Puller (P-97, Sutter Instruments, San Rafael, CA, USA). Electrode resistance was 20–40 MΩ when filled with 1 M KCl and 30–80 MΩ when the electrode tip contained Ca^{2+} dye and caged Ca^{2+} (see below). Electrode signals were amplified with an Axoclamp 2A (Axon Instruments, Foster City, CA, USA) operated in bridge mode and sampled at rates of 3 or 4 kHz with an amplitude resolution of 0.0244 mV by an analog-to-digital converter (DT2801A, Data Translation, Marlboro, MA, USA). Recording duration was approximately 10–40 min.

Measurements of the neuronal input resistance (R_{in}) were performed by probing the neurons' responses to rectangular current pulses of 80 ms duration. Hyperpolarizing currents of small amplitude (−1 nA) were used to minimize the involvement of active currents (Haag et al., 1997). A linear relationship between injected current and resulting voltage was found to hold for TCs in the hyperpolarized voltage range (Borst and Haag, 1996). Bridge recording mode was used instead of discontinuous current clamp (DCC) to measure R_{in}, since the same current level was used for all injections. In this case, DCC would provide no advantages over bridge mode but would add more noise to the recording. The bridge balance was precisely calibrated to the −1 nA current injections. The average membrane potential was determined in 60 ms time windows centered on phases with and without current injection. For each time window with current injection the membrane potential values were subtracted from the average value of the two neighboring time windows without current injection and R_{in} values were calculated according to Ohm's law. Under- and overcompensation of the electrode's resistance by the amplifier's bridge circuit might have led to over- and underestimation of R_{in} values. Such electrode compensation errors would leave the es-

timation of sign and amplitude of changes in neuronal R_{in} unaffected. Note however, that when plotting R_{in} changes relative to resting values, electrode over- and under-compensation would lead to over- or underestimation of relative resistance changes, respectively. Such errors are small when R_{in} changes are small in relation to resting values as is the case for R_{in} changes after the cessation of motion stimulation (see Results). Moreover, the magnitude of measured R_{in} changes might depend on impalement site. Since the electrode was placed in the axon, R_{in} changes located in the dendrite might have been underestimated. However, the classes of TCs recorded in this study possess large axon diameters of 10–25 μm (e.g. Hausen, 1982). In a compartmental model study on these TCs 20–80% of current injected into the axon was estimated to reach the dendritic tips (depending on TC class, see Borst and Haag, 1996).

UV photolysis of caged Ca^{2+} and Ca^{2+} imaging

Photolysis of caged Ca^{2+} and Ca^{2+} imaging followed Kurtz (2004), apart from some minor modifications as detailed below. Caged Ca^{2+} and fluorescent Ca^{2+} dye was injected from the electrode tip into single TCs during intracellular recording by applying 1–3 nA hyperpolarizing current for 5–10 min and left to diffuse throughout the cytoplasm for $\geq$5 min. The electrode tips contained 5 mM KOH and 101–127 mM o-nitrophenyl EGTA (NP-EGTA) tetrapotassium salt and 5–6 mM Oregon Green 488 1,2-bis(o-aminophenoxy)ethane-N,N,N',N'-tetraacetic acid (BAPTA)-1 hexapotassium salt (both from Molecular Probes, Eugene, OR, USA; concentration ranges indicate variations between experiments). With this procedure, step-like increases of the cytosolic Ca^{2+} concentration could be induced repetitively by delivering filtered light ($\lambda<360$ nm or $\lambda<380$ nm) from a xenon flash lamp (JML-C2, Rapp Optoelectronics, Hamburg, Germany) via a quartz light guide (diameter 100 or 200 μm). In addition to UV flashes, continuous illumination with filtered light ($\lambda<360$ nm) from a UV lamp (UVICO, Rapp Optoelectronics) was used to release caged Ca^{2+}. Due to the fly's photoreceptors' sensitivity to UV light (Kirschfeld and Franceschini, 1977), visual responses are observed in TCs during UV photolysis of caged Ca^{2+}. I applied two kinds of controls to distinguish cellular responses, which are elicited by increases in the cytosolic Ca^{2+} concentration from those elicited by unwanted visual stimulation. First, I recorded control traces with UV illumination before injection of caged Ca^{2+}. Alternatively, the flash or continuous-light lamp system was used with long-wavelength filtering ($\lambda>475$ nm). This filtering produced equally strong visual excitation but no photorelease of caged Ca^{2+}.

Relative cytosolic Ca^{2+} concentration changes in single TCs were monitored by epifluorescence imaging of Oregon Green 488 BAPTA-1 emission. I used long working-distance objectives (Achroplan 20× NA 0.50W and 40× NA 0.75W, Zeiss) at an upright fixed-stage microscope (Axioskop FS, Zeiss; filter settings: excitation 475±20 nm, dicroic mirror 500 nm, emission 530±20 nm) equipped with a cooled frame-transfer charged-coupled device (CCD) camera (Quantix 57, Photometrics, Tucson, AZ, USA), operated with 4×4 pixel binning at a frame rate of 14 Hz.

Visual stimulation and data analysis

A light emitting diode board was used to present a moving high-contrast square wave grating in the receptive field of TCs (for details see Kurtz et al., 2001). The angular extent of the pattern was approximately 50×60°, with the larger extent perpendicular to the axis of motion. The temporal frequency of pattern motion was 4 Hz.

Ca^{2+} concentration signals were evaluated as fluorescence changes of the Ca^{2+}-sensitive dye relative to resting values obtained from the first image ($\Delta F/F$). Background values were calculated by averaging the signal from unstained regions in the

images and subtracted from the values in the regions-of-interest. This procedure adds noise to the $\Delta F/F$ time courses, but improves the comparability of Ca^{2+} concentration signals from regions with different staining intensity.

Routines written in C (Borland, Scotts Valley, CA, USA) were used to control visual stimulation and electrophysiological data acquisition. PMIS (GKR Computer Consulting, Boulder, CA, USA) was used for CCD camera control and image analysis. Matlab (The Mathworks, Natick, MA, USA) was used for data analysis. Unless otherwise mentioned, all values are given as mean±standard deviation. The lowercase letter n denotes the number of measurements from one cell, uppercase N denotes the number of cells.

RESULTS

Direction-selective and direction-unselective components of motion adaptation

Prolonged exposure to visual motion leads to a strong reduction of the response amplitude of TCs, which are visual motion-sensitive neurons of the fly brain. During the first few hundreds of milliseconds after motion onset, part of this reduction can be attributed to the correlation-based mechanism of motion detection, which inherently generates a transient response characteristic (Egelhaaf and Borst, 1989; Borst et al., 2005). Later on, however, changes in gain or filtering properties are most likely responsible for further decreases in response amplitude. Such changes have been termed adaptation, since they seem to shift the operating range of the neuron to currently prevailing stimulus intensities or help to save energy (review: Clifford and Ibbotson, 2002).

In Fig. 1 the membrane-potential responses of one class of TC, a "vertical system" neuron (VS2 or VS3-cell), are shown. The neuron is exposed to movement of a high-contrast square-wave grating in either the neuron's PD, downwards, or in the opposite direction, the so-called null direction (ND). Different durations of PD motion are followed by 0.5-s presentation of the stationary grating and 1 s during which the stimulus moves again, providing a test stimulus to assess the strength of motion adaptation. The axonal response of VS-cells to PD motion is a graded depolarization with superimposed "spikelets," Na^+-current driven depolarizing transients of variable amplitude (Hengstenberg, 1977, 1982). After less than 5 s of motion, the neuron's voltage response was reduced to a low steady-state value (Fig. 1A). Accordingly, the response to the 1-s test stimulus was much weaker after long-lasting adaptation than in the unadapted state (compare top left with bottom panel in Fig. 1A).

Adaptation of a neuron might result from an activity-dependent control of the response gain in the neuron itself (e.g. Sanchez-Vives et al., 2000a). Alternatively, decreases in the neuron's response might reflect adaptation of elements presynaptic to the neuron rather than intrinsic adaptation (e.g. Manookin and Demb, 2006). The response to the 1-s PD test stimulus was attenuated by preceding long-lasting ND adaptation almost as much as by PD adaptation (see Fig. 1A and B). Since PD and ND motion leads to membrane potential deflections of opposite sign, it can be ruled out that adaptation is exclusively controlled in an activity-dependent manner by the preceding
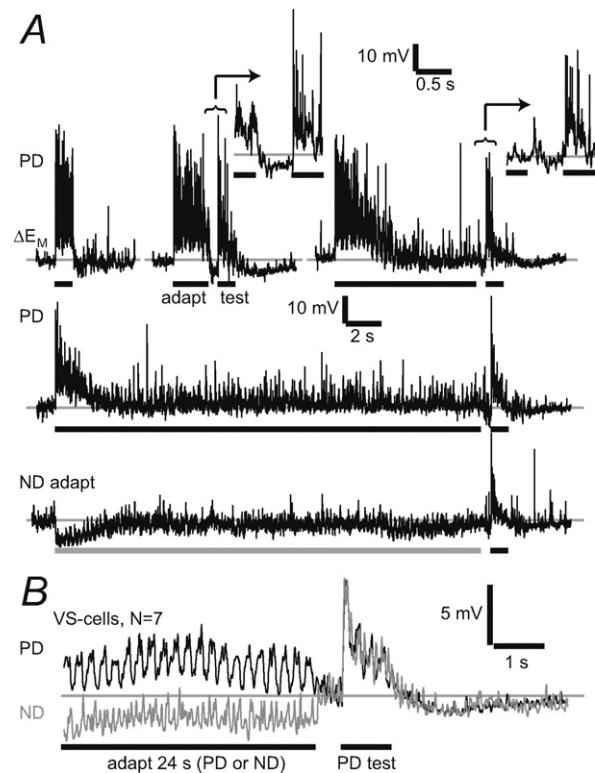
Fig. 1. Adaptation of the membrane-potential responses of a visual motion-sensitive neuron in the fly brain (VS-cell) to various motion durations. (A) As a test stimulus a high-contrast square-wave grating moves in the receptive field of the VS-cell in the preferred motion direction, i.e. downward (PD). The test stimulus is presented alone (upper trace, left) or 0.5 s after the presentation of an adapting stimulus, consisting of 2, 8 or 24 s of motion. The 24-s stimulus was presented in PD or ND (ND adapt). The test stimulus always moves in PD. The insets show excerpts (as indicated by the parentheses) on a finer time scale from conditions with 2-s and 8-s adaptation to illustrate that the AHP is stronger after 2 s than after 8 s of adapting motion. Gray horizontal lines indicate baseline levels determined for each trace as the mean over an interval 26.5–24.5 s before the onset of test motion. (B) Comparison of the test responses after 24 s of motion in either PD (black) or ND (gray). Mean traces for seven VS neurons, smoothed by a rectangular filter with 20 ms bin width. The responses to test motion have similar amplitudes after adaptation in PD and ND, although the responses during the adapting phase differ in their sign. This indicates strong direction-unselective adaptation after long-lasting motion presentation.

ing level of neuronal excitation of the TC itself. More probably, the strong adaptation after long-lasting motion stimulation results mainly from elements in the motion-detection pathway *before* the calculation of direction-selectivity. Otherwise, adaptation in one direction would leave the response to stimuli moving in the opposite direction unaffected, which was clearly not the case.

Although direction-unselective components seemed to dominate adaptation after tens of seconds of motion stimulation, indications of direction-selective motion adaptation were also present: as is most clearly visible after PD motion stimulation of medium duration (see e.g. the condition with a 2 s adapting stimulus in Fig. 1A), a hyperpolarizing shift in the membrane potential, an AHP, followed cessation of motion stimulation (Fig. 1A, inset in middle

panel). The fact that the AHP was more pronounced after several seconds than after several tens of seconds of PD motion (compare insets of top middle and top right panel in Fig. 1A) suggests that this effect is regulated by the activity of the neuron itself: after longer motion stimulation the activity of the neuron had run down to a large extent, leading to less activity-dependent AHP than after shorter motion stimulation. The idea of an activity-dependent control of AHP is corroborated by the fact that it is not symmetric with respect to the direction of motion-stimulation: no analogous effects are observed after ND stimulation (Harris et al., 2000; Kurtz et al., 2000; see also Fig. 2A).

The correlation between motion direction and AHP and the impact of AHP on the response to subsequent motion stimuli has already been analyzed in detail by Harris et al. (2000) and Kurtz et al. (2000) and for that reason was not investigated here. However, it is still an open question whether the AHP results from mechanisms intrinsic to TCs or presynaptic to them. It is plausible to suggest that the AHP results from activation of an inhibitory ionic membrane conductance, e.g. Ca^{2+}-dependent K^+-channels. There exists, however, an alternative explanation of how a membrane hyperpolarization may be generated in a motion direction-selective way: TCs receive input from excitatory and inhibitory presynaptic elements, probably through acetyl cholinergic and GABAergic synapses, respectively (Single et al., 1997; Oertner et al., 2001). Ongoing PD motion might lead to a depression of excitatory inputs over time. Since the input channels are assumed to be tonically active during rest, slow recovery from such a depression would then lead to a hyperpolarization after cessation of PD motion. To account for the fact that ND motion is not followed by a marked after-depolarization, it would have to be claimed that the depression of the inhibitory input is either less pronounced or recovers faster.

Input-resistance changes accompanying the AHP in TCs

To find out whether direction-selective adaptation is generated by activation of a conductance in the TC itself or by depression of one type of its input channels, I measured changes in neuronal R_{in} during and after motion stimulation. If the AHP following PD motion were due to depression of inputs, it should be accompanied by an increase in R_{in}. In contrast, a decrease in R_{in} would hint at an activity-regulated ionic conductance, such as Ca^{2+}-dependent K^+-channels. Since the two proposed mechanisms are not mutually exclusive, the AHP might also be produced by a mixture of both mechanisms. In this case, no clear predictions can be made for R_{in}.

Fig. 2A shows membrane potential recordings from a horizontal system equatorial (HSE)-cell, a TC which responds to motion in a similar way as VS-cells, although it has a different PD: horizontal system (HS)-cells are sensitive to horizontal motion, being depolarized during front-to-back motion and hyperpolarized during back-to-front motion in the ipsilateral field of view (Eckert, 1981; Hausen, 1982). Similar to VS-cells (see Fig. 1), depolarizing responses of HS-cells are followed by an AHP,
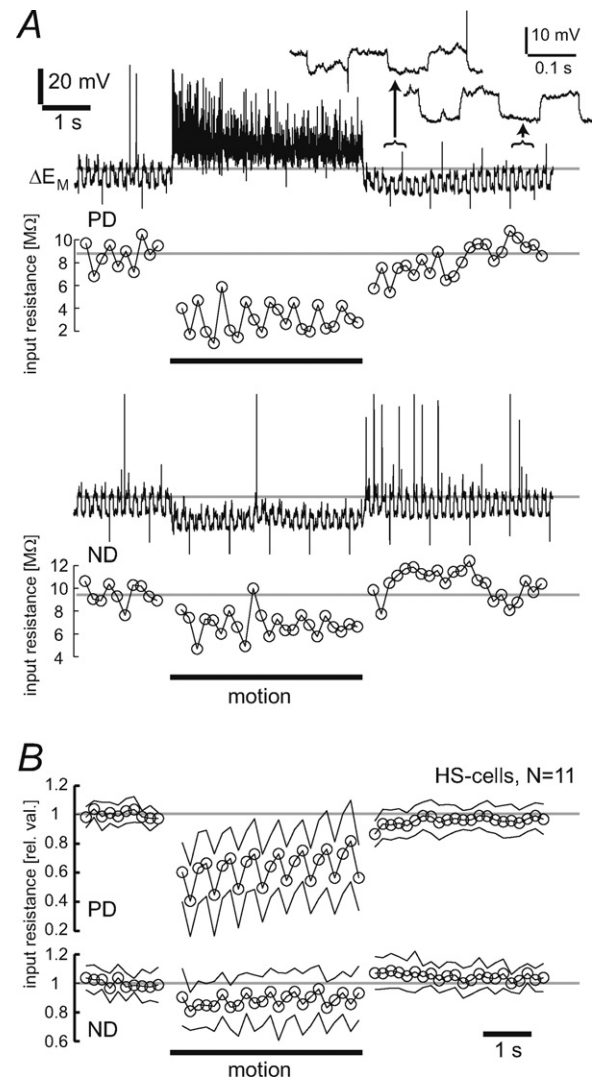
Fig. 2. Changes in neuronal R_{in} induced by motion in PD and ND. (A) Measurement of R_{in} of an HSE neuron by injection of hyperpolarizing rectangular current pulses (-1 nA) before, during and after presentation of motion the PD (top) and in the ND (bottom). Shown are the membrane potential responses and the calculated R_{in} values. Gray horizontal lines indicate resting levels, determined for the membrane potential traces as mean values in phases without current injection in a 2-s time window before motion onset and for R_{in} as average over 10 data points prior to stimulation (1.76–0.26 s before motion onset). R_{in} decreases both during PD and during ND motion and remains decreased after PD motion. The insets illustrate that the decrease in R_{in} after PD motion, concomitant with the AHP, is expressed in an attenuated response to the test current pulses. After ND motion R_{in} is elevated relative to its resting level. (B) Time courses of R_{in} before, during and after presentation of motion in the PD (top) and in the ND (bottom). Average values for 11 HS-cells (dots, mean; lines, standard deviation).

whereas at most very small after-potentials occur after cessation of ND motion (Harris et al., 2000; Kurtz et al., 2000; see also Fig. 2A). To assess changes in R_{in} during and, in particular, after motion stimulation, I injected square pulses of 1 nA hyperpolarizing current into TCs (see Experimental Procedures for details). In the example cell shown in Fig. 2A, the response to PD motion was

accompanied by a strong reduction in R_{in} from a resting value of 9.0 ± 0.5 MΩ to 3.6 ± 0.5 MΩ ($n=5$, time window $0.24-3.75$ s after motion onset), which was a reduction to 40% of the resting value (determined as mean value over $1.76-0.26$ s before motion onset). During ND motion the R_{in} was reduced from 9.6 ± 0.2 MΩ to 6.7 ± 0.2 MΩ ($n=3$), equivalent to 70% of the resting value. Such relatively low resting R_{in} values and the strong reductions in R_{in} during both PD and ND motion are in accordance with previous studies on fly TCs (Borst and Haag, 1996; Single et al., 1997). The reductions in R_{in} during visual motion have been concluded to be largely a consequence of the activation of increased excitatory and inhibitory synaptic input activity (Borst and Haag, 1996; Single et al., 1997). Similarly strong stimulation-induced changes in neuronal R_{in}, which are strongest during PD but marked during ND stimulation as well, have been described in cat visual cortex neurons (Anderson et al., 2000). The mean changes in R_{in} during PD and ND motion were determined for HS-cells and averaged over different cells. R_{in} decreased to 64 ± 17% and 88 ± 14% ($N=11$) of the resting values during PD motion and ND motion, respectively. The larger magnitude of input-resistance decreases during motion in PD in comparison to ND is not surprising, since motion in PD activates, in addition to the synaptic conductances, voltage-dependent conductances in the TC leading to the generation of spikelets (Haag et al., 1997, see also Fig. 2A). The activation of voltage-dependent conductances may be phase-coupled to the temporal frequency of pattern motion, which would explain why strong modulations in R_{in} often occur during motion in PD but not during motion in ND (see Fig. 2).

After cessation of motion in PD, but not after ND motion, R_{in} remains below its resting value for about 1–2 s. For the example HSE-cell, R_{in} averaged over a 2-s time window starting 0.26 s after cessation of motion was decreased to 94 ± 7% ($n=5$) of its resting value. In contrast, after ND motion R_{in} was increased to 108 ± 7% ($n=3$). The reduction of R_{in} after PD motion supports the hypothesis that the AHP is not due to a long-lasting depression of excitatory inputs, but is instead the consequence of the activation of an ionic conductance, such as Ca^{2+}-dependent K^{+}-channels. The corresponding average values for the tested 11 HS-cells were 95 ± 8% and 105 ± 5% for PD and ND, respectively. In Fig. 3 these data are plotted together with data from five additional HS neurons for which only PD responses were recorded and with data from VS-cells and from CH-cells (centrifugal horizontal cells). The latter type of neuron is an inhibitory interneuron receiving input from HS-cells via dendrodendritic synapses (Haag and Borst, 2002). In contrast to HS and VS-cells, CH-cells generate purely graded membrane potential responses without superimposed spikelets (Eckert and Dvorak, 1983). The data from the entire cell sample corroborate the findings obtained from the HS-cell sub-sample: R_{in} dropped strongly during PD motion and less pronounced during ND motion. After the cessation of PD motion R_{in} stayed below its resting value, whereas, at least in HS-cells, it was slightly elevated after ND motion. Rel-
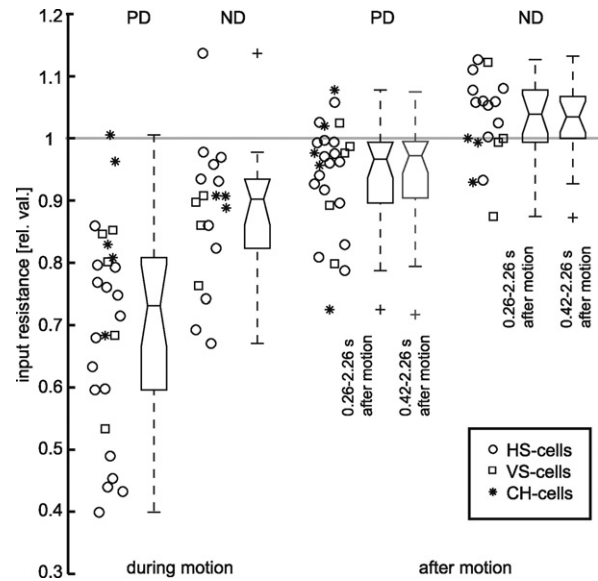
Fig. 3. R_{in} values during and after motion relative to resting levels. For the ND 11 HS-cells, four VS-cells and three CH-cells were measured. For the PD the data set comprised the same neurons and additional five HS-cells, one VS-cell and two CH-cells. The symbols represent mean values from single neurons, with different symbol types for the different cell classes. The number of data traces recorded per neuron ranged from $n=1$ to $n=8$ (median $n=3$) for PD and $n=1$ to $n=8$ (median $n=2$) for ND. For display reasons, the symbols are scattered along the x axis. The box-whisker plots show the distribution of the mean values obtained for each neuron. Horizontal lines of the boxes indicate the lower quartile, median and upper quartile values. The whiskers show the extent of the rest of the data. Maximal whisker length is 1.5 times the inter-quartile range. Data values beyond the end of the whiskers are classified as outliers and are displayed as a cross. Notches provide an estimate of the uncertainty about the means for box-to-box comparisons: the medians are significantly different ($P<0.05$) if the corresponding notches do not overlap. During motion, R_{in} values were averaged over a time window 0.24–3.75 s after motion onset. To evaluate the after-response in R_{in}, we averaged over a time window 0.26–2.26 s after cessation of motion. The first data point after cessation of motion often shows a more pronounced change in R_{in} than the following values (see Fig. 2B). To rule out that my conclusions depend critically on inclusion of this data point box-whisker plots were also calculated for a time window excluding this data point (0.42–2.26 s after motion stop). Accordingly, the statistical significance levels of deviations of the data from one (see text) were equal for both time windows.

ative R_{in} values were significantly different from one after PD motion (Wilcoxon signed rank test, $P<0.05$), but not after ND motion ($0.1>P>0.05$), although in the latter condition statistical significance was reached for the subgroup of HS neurons ($P<0.05$). Accordingly, the relative R_{in} values after PD motion were significantly different from those after ND motion (Wilcoxon rank sum test, $P<0.001$). The R_{in} elevation after ND motion could be due to the fact that the conductance leading to AHP is tonically active during rest, suppressed during ND motion and slowly recovering after cessation of ND motion. This idea is, however, not easily compatible with the finding that ND motion was not followed by a marked after-depolarization (Kurtz et al., 2000; Harris et al., 2000). Alternatively, given the fact that during motion in the ND not only inhibitory but also excitatory inputs are activated to a certain extent (Single et al.,

1997), a balanced depression of both kinds of synaptic inputs after stimulation might lead to an increase in R_{in} in the absence of prominent changes in membrane potential. Note, that such a synaptic depression would then also occur after PD motion and that it would increase R_{in}. Since this increase in R_{in} would counteract the decrease elicited by an activity-dependent conductance, the amplitude of the latter would be underestimated in our measurements. Altogether, these findings corroborate the conclusion that the direction-selective component of adaptation, which expresses itself in the form of an AHP, is based on an activity-dependent mechanism intrinsic to TCs, for example activation of Ca^{2+}-dependent K^+-channels.

UV-photolysis of caged Ca^{2+} in TCs

Physiological mechanisms of adaptation intrinsic to TCs have to account for two prominent features of adaptation: first, adaptation mainly occurs if adapting motion and test motion are presented at the same location within the large spatial receptive field of the TC (Maddess and Laughlin, 1985; but see also: Neri and Laughlin, 2005). Second, the time courses of the buildup of and recovery from adaptation resemble a temporally low-pass-filtered version of the membrane potential. Thus, the adaptational state of a TC is shaped by several seconds of stimulus history. Intracellular Ca^{2+} has been proposed to mediate direction-specific adaptation in TCs, since it meets both demands: first, the dendritic Ca^{2+} concentration rises during PD motion and Ca^{2+} signals remain locally restricted to those parts of the dendrite, which receive retinotopic input (Borst and Egelhaaf, 1992; Dürr and Egelhaaf, 1999). Second, Ca^{2+} accumulation in the cytosol during excitatory stimulation and its subsequent clearance resembles the time course of direction-specific adaptation (Kurtz et al., 2000).

Since the magnitude and time course of Ca^{2+} accumulation are correlated with the AHP following PD motion, a Ca^{2+}-dependent inhibitory conductance has been proposed to form the physiological basis of locally regulated direction-selective adaptation (Kurtz et al., 2000). The changes in R_{in} described in the present account, in particular the declines in R_{in} after PD motion, are in accordance with this hypothesis. Therefore, I tested whether rises in cytosolic Ca^{2+} without concomitant visual stimulation exert direct effects on the membrane potential or on R_{in} of TCs (Fig. 4). The cytosolic Ca^{2+} concentration was artificially raised by filling single TCs with caged Ca^{2+} (NP-EGTA) and exposing the neuron to constant UV light (Fig. 4A) or to a brief UV flash (Fig. 4B). With these techniques, rises in the cytosolic Ca^{2+} concentration were obtained throughout the neuron, with concentration signals similar in their peak amplitude to those after several seconds of visual PD motion of a high-contrast pattern, a stimulation that has been shown to elicit pronounced AHP (Harris et al., 2000; Kurtz et al., 2000). Due to the limited duration of *in vivo* imaging experiments and pre-existing knowledge about visual Ca^{2+} responses, in the present study Ca^{2+} signals during visual stimulation were not systematically recorded and compared with Ca^{2+} signals elicited by UV photolysis. However, for the subset of TCs where such comparisons

were made, the Ca^{2+} signals were in all but one case larger after UV photolysis than after 4 s of visual stimulation ($N=14$ HS-cells, 2 VS-cells, 12 CH-cells). After UV photolysis, the spatially averaged background-subtracted Ca^{2+} signals at TC dendrites (as shown in Fig. 4) reached an amplitude of $24.7\pm23.3\%$ ($N=34$, mean value over all cell classes and conditions). This value exceeds those obtained in previous studies using visual stimulation and Ca^{2+} indicator dyes with similar properties (Egelhaaf and Borst, 1995; Single and Borst, 1998, 2002). Moreover, in the majority of my experiments imaging of Ca^{2+} release by UV photolysis was performed after examining the effects of Ca^{2+} release on the electrical properties of the neuron. This may have led to underestimation of the actual Ca^{2+} release during the electrophysiological investigation because of depletion of caged Ca^{2+} upon repeated UV illumination. Therefore I conclude that the bulk cytosolic Ca^{2+} concentration levels reached by UV photolysis of caged Ca^{2+} were usually higher than those after several seconds of visual stimulation. Notwithstanding, during visual stimulation near-membrane Ca^{2+} might rise much faster and might reach higher concentration levels. Note however, that adaptation is correlated in its strength and its time course with the Ca^{2+} concentration signal as measured with wide-field fluorescence microscopy, i.e. bulk cytosolic Ca^{2+} rather than near-membrane Ca^{2+} (see Discussion).

UV illumination elicits depolarizations in TCs, since it penetrates the fly head and excites the photoreceptors, which are in the fly sensitive to UV wavelengths (Kirschfeld and Franceschini, 1977). To dissociate effects produced by unwanted visual stimulation from those produced by Ca^{2+}, long-wavelength illumination ($\lambda>475$ nm), which elicits similar depolarizations but does not lead to photolysis of caged Ca^{2+}, was used as a control (see Fig. 4C). Alternatively, control traces were recorded in which UV illumination was applied prior to the iontophoretic application of caged Ca^{2+}. Fig. 4C shows an example membrane potential recording during photolysis of caged Ca^{2+} by constant UV-illumination and the corresponding control trace for the same HSE-cell as shown in Fig. 4A. There is no obvious membrane hyperpolarization similar to the AHP, as would be expected to follow UV photolysis of caged Ca^{2+} if Ca^{2+}-dependent K^+-channels or any other Ca^{2+}-dependent inhibitory conductance were activated. For the same neuron as shown in Fig. 4B R_{in} was measured during UV flash-photolysis of caged Ca^{2+} (Fig. 4D). Neuronal R_{in} appeared unaffected by the control flashes (applied before filling the neuron with caged Ca^{2+}) as well as by actual Ca^{2+} release.

To quantify the above observations, mean membrane potential changes relative to the resting potential as well as mean changes in R_{in} were determined after UV photolysis of caged Ca^{2+} and after control illumination for a number of TCs. Neither flash photolysis of caged Ca^{2+} nor photolysis by constant UV illumination led to membrane hyperpolarization (Fig. 5A). In contrast, a weak depolarization was observed after UV illumination (Wilcoxon signed rank test, $P<0.05$), whereas in the control condition a non-significant tendency to hyperpolarize was present

Fig. 4. UV-photolysis of caged Ca^{2+} in TCs. (A) Fluorescence measurements of dendritic Ca^{2+} signals during PD motion and during artificial Ca^{2+} release. An HSE-cell was filled with the photolabile Ca^{2+} chelator NP-EGTA and the Ca^{2+}-sensitive dye Oregon Green 488 BAPTA-1. The relative Ca^{2+} concentration signal ($\Delta F/F$) obtained from a dendritic region rises during PD motion (black data trace) and in response to illumination with constant UV light (red data trace, data points during UV illumination have been blanked). The dendrite of the HSE-cell is visible in the raw fluorescence image. The color-coded images (see B for color code of $\Delta F/F$) illustrate Ca^{2+} fluorescence before stimulation (open asterisk), and at the peaks of the time courses during UV photolysis (closed red asterisk) and during visual stimulation (closed black asterisk). In the images the irregular-shaped regions used for quantification of the fluorescence signal (colored area) and for background subtraction (white area) are depicted. (B) Ca^{2+} concentration signals at the dendrite of a DCH-cell (dorsal CH neuron) during visual stimulation and after photolysis of caged Ca^{2+} by a UV flash. Data presentation as in A. (C) Membrane potential changes recorded from the HSE-neuron shown in A during UV photolysis of caged Ca^{2+} and during a control illumination with long-wavelength light. Under both conditions, a primarily depolarizing membrane potential response results from penetration of excitation light through the fly's head and excitation of the photoreceptor layer. In the example trace shown, the light-induced depolarization is slightly stronger during UV illumination than during long-wavelength illumination. This was also true for the average values (1.81 ± 1.46 versus 1.12 ± 1.01 mV during 1 s of UV and long-wavelength illumination, respectively, $N=24$). In spite of the fact, that this discrepancy might lead to an overestimation of UV-induced effects, a prominent AHP following photorelease of Ca^{2+} is not present (see also Fig. 5A). (D) R_{in} relative to resting level during UV flash photolysis of caged Ca^{2+} (upper trace, $n=8$) and in two control experiments (lower traces), in which the UV flash was applied prior to the iontophoretic application of caged Ca^{2+}. The photorelease of Ca^{2+} does not elicit a prominent decrease in neuronal R_{in}.

($0.1 > P > 0.05$). Both effects are weak with median amplitudes of less than 0.5 mV and might reflect differential effects of visual stimulation by UV and long-wavelength light.

In accordance with the absence of an AHP after photorelease of Ca^{2+} consistent decreases in R_{in}, as would be indicative of a Ca^{2+} regulated inhibitory conductance, were not measured (Fig. 5B). Although, over the entire sample of neurons a slight, non-significant reduction in R_{in} was present (Wilcoxon signed rank test, $P > 0.1$), this was most probably not a consequence of photorelease of Ca^{2+}, since the reduction in R_{in} was even more pro-

nounced in the control condition (relative R_{in} was significantly different from 1, $P < 0.05$).

In light of the above results, it would appear highly unlikely that photorelease of Ca^{2+} would affect motion responses in a similar way as adapting motion. To be on the safe side, I tested experimentally whether photorelease of Ca^{2+} affects the response to a subsequently presented motion stimulus (see Fig. 6). If Ca^{2+} directly exerted effects similar to direction-selective motion adaptation, the response to PD motion would be attenuated (Kurtz et al., 2000). This effect would be expected to be most pronounced at the beginning of the motion response,

Fig. 5. Membrane potential changes and R_{in} relative to resting level after UV-photolysis of caged Ca^{2+} and after control illumination. (A) Deviation of the mean membrane potential (averaged over 0.20–2.20 s after illumination) from the resting value (2-s time window before illumination). Each symbol represents one individual neuron of a certain class, as specified in the inset to B. In total, for 16 HS, 14 CH and two VS neurons responses were determined both to UV-photolysis of caged Ca^{2+} and to control illuminations. The number of data traces per neuron ranged from $n=1$ to $n=14$ (median $n=3$) in photolysis experiments and from $n=1$ to $n=11$ (median $n=4$) in control experiments. Data from the two types of control, UV illumination before application of caged Ca^{2+} and long-wavelength illumination were pooled, since no obvious differences were observed. The type of experiment was as follows: open symbols, flash illumination; closed black symbols, 1-s constant illumination; closed gray symbols, 3-s constant illumination. For calculation of box-whisker plots, data from all types of experiments and all cell classes were pooled. See Fig. 3 for details on box-whisker plots. (B) R_{in} after UV flash photolysis of caged Ca^{2+} (time window 0.26–2.26 s after illumination) relative to resting level (1.76–0.26 s before illumination) and in corresponding control experiments. In total, for eight HS neurons, eight CH neurons and one VS neuron responses were determined both to UV-photolysis of caged Ca^{2+} and to control illuminations. Additionally, two CH neurons for which only the photolysis condition but not the control was recorded are included. The number of data traces per neuron ranged from $n=2$ to $n=7$ (median $n=5$) in photolysis experiments and from $n=3$ to $n=7$ (median $n=5$) in control experiments. Presentation of data as in A.

because later on direction-unselective adaptation is most influential on the motion response. Averaged over a 0.3-s time window starting 50 ms after motion onset, the amplitude of the motion response was 8.1±0.4 mV ($n=6$) in the control condition and 8.4±0.9 mV ($n=5$) after photorelease of Ca^{2+}. Thus, motion responses were not attenuated by artificially increased cytosolic Ca^{2+} concentration levels.

In summary, release of caged Ca^{2+} led neither to membrane hyperpolarization, nor to a decrease in neuronal R_{in}. Accordingly, motion stimuli presented after photorelease of Ca^{2+} were not attenuated, speaking against the earlier hypothesis that direction-selective adaptation in TCs is regulated by the concentration of bulk cytosolic Ca^{2+} (Kurtz et al., 2000).

DISCUSSION

Adaptation is an ubiquitous phenomenon of electrically excitable cells, ranging from the primary processing stages (e.g. photoreceptors, for review see Fain et al., 2001; auditory hair cells, for review see Fettiplace and Ricci, 2003) to neurons in higher-order brain areas (e.g. Chung et al., 2002; Ibbotson et al., 1998; Kohn and Movshon, 2004; Tolias et al., 2001; Huk et al., 2001). In particular for neurons performing higher-order functions, like complex visual-motion analysis, it is often impossible to find out whether adaptation is based on mechanisms in these neurons themselves or whether it originates in more peripheral processing stages. In the present study, I could unravel the origin of direction-selective adaptation as being intrinsically
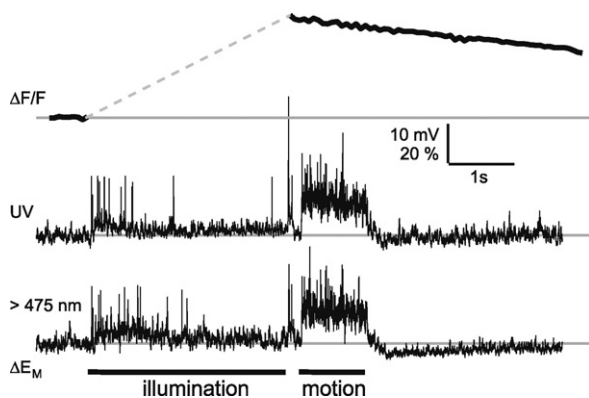
Fig. 6. Motion response after Ca^{2+} photorelease and after control illumination. A 3-s UV illumination elicited a large increase of the Ca^{2+} fluorescence signal ($\Delta F/F$) averaged over the dendrite of an HSE-cell (upper trace). The response to a 1-s PD motion stimulus presented 200 ms after illumination is shown for the condition with Ca^{2+} photorelease ($\Delta F/F$ and ΔE_M recorded non-simultaneously) and for the control condition with long-wavelength light.

generated in fly motion-sensitive neurons, the TCs. This conclusion is built on the finding that R_{in} of TCs decreases after PD motion stimulation. This decrease coincides with the generation of an AHP and is indicative of an activity-regulated ionic conductance. In contrast, another component of adaptation seems to be based on the depression of the activity of presynaptic neurons, since, at least in HS-cells, an elevated R_{in} was found after motion in ND.

I tested the involvement of Ca^{2+} in direction-selective adaptation directly by the photorelease of caged Ca^{2+} in single TCs. Unlike many other types of neurons in which the activity-dependent control of ionic conductances is mediated by Ca^{2+} (e.g. Lancaster et al., 1991; Schwindt et al., 1992; Osmanovic and Shefner, 1993; Lancaster and Zucker, 1994; Kurahashi and Menini, 1997; Sanchez-Vives et al., 2000a), the activity-dependent conductance increase in TCs seems not to be regulated by Ca^{2+}, because even large concentration steps in cytosolic Ca^{2+} did neither lead to AHP nor to detectable conductance increases.

Methodological considerations

The decreases in R_{in} after PD motion were fairly weak in comparison to those during motion stimulation. Is a 5% decrease in R_{in} really sufficient to explain AHPs with peak amplitudes of up to -3 mV? This might appear implausible, since R_{in} changes during motion stimulation were much stronger (up to 60%). A plausible reason for the comparatively weak changes in R_{in} after motion stimulation is that the adaptation-induced decrease in R_{in} is to some extend counteracted by another adaptation process which leads to an increase in R_{in}. This is suggested by the presence of increases in R_{in} after adaptation with motion in ND. These increases in R_{in} are most probably due to an adaptation-induced depression of the activity of synaptic inputs or of synaptic gain. Thus, adaptation might be based on several mechanisms, which have opposite influence on R_{in}, and which lead to a net increase in R_{in} after ND motion but to a net decrease in R_{in} after PD motion.

In view of these considerations, artificial elevation of the cytosolic Ca^{2+} concentration by UV-photolysis of caged Ca^{2+} could be expected to cause marked R_{in} decreases and AHP, if direction-selective adaptation were mediated by Ca^{2+}. This was not observed in my study, despite the fact that fluorescence monitoring of cytosolic Ca^{2+} signals indicated higher peak concentrations after photolysis than after visual stimulation. It might be argued that the much higher concentration levels to which Ca^{2+} rises directly at the cell membrane near open Ca^{2+} channels evade detection by fluorescence microscopy. Ca^{2+} concentrations obtained by UV photolysis might therefore be too low to cause adaptation. This argumentation is, however, not easily compatible with the fact, that the adaptational state follows a low-pass-filtered (i.e. temporally integrated) version of the membrane potential. Only the slow and sustained changes of bulk cytosolic Ca^{2+} accumulation, but not the fast changes in near-membrane Ca^{2+} concentrations would represent such a low-pass-filtered signal. Accordingly, in TCs the time course of the buildup of the AHP with motion stimulation was found to resemble that of the bulk cytosolic Ca^{2+} concentration (Kurtz et al., 2000). Nevertheless, fast changes in near-membrane Ca^{2+} concentrations could in principle result in an AHP with slow kinetics, if long delays in the regulation of an underlying Ca^{2+}-dependent channel were present both after binding and after unbinding of Ca^{2+}. Such slow kinetic regulation seems not to exist in apamin-sensitive Ca^{2+}-regulated K^{+}-channels (Gurney et al., 1987). Likewise, in BK-channels the Ca^{2+}-dependent regulation is so fast, that currents through these channels can even be used to track fast Ca^{2+} dynamics (Yazejian et al., 2000). In contrast, a discrepancy between the time course of Ca^{2+} concentrations and that of the activity of apamin-insensitive Ca^{2+}-regulated K^{+}-channels has been demonstrated (Sah and Clements, 1999). Since it is largely unknown which types of Ca^{2+}-regulated K^{+}-channels exist in insect neurons, it is at present not possible to resolve whether a slowly varying AHP might be controlled by the fast fluctuations in near-membrane Ca^{2+} concentration instead of by the much slower changes in bulk cytosolic Ca^{2+} concentration.

In the present study, some TCs showed fairly weak Ca^{2+} responses during visual stimulation. A possible reason may be buffering of cytosolic Ca^{2+} by free NP-EGTA. It might be argued that due to this high buffering capacity even after UV photolysis Ca^{2+} remained below the concentration levels necessary to induce adaptation. This objection does, however, not agree with the fact that a marked AHP after PD motion persisted if cells were filled with NP-EGTA. Moreover, as mentioned in a previous study, the AHP was not abolished by the iontophoretic injection of the high-affinity Ca^{2+}-buffer BAPTA into single TCs (Kurtz et al., 2000).

Which ionic mechanisms might underlie intrinsic direction-selective adaptation in TCs?

It is improbable, that the AHP is generated by purely voltage-gated channels with slow enough deactivation kinetics to cause significant long-lasting hyperpolarization following depolarizing stimulation, because in voltage-clamp experiments deactivation of outward currents was found to be in the range of several tens of milliseconds (Haag et al., 1997). Thus it is most plausible to assume that direction-selective adaptation is mediated by an activity-dependent messenger other than cytosolic Ca^{2+}. In their voltage-clamp experiments Haag et al. (1997) segregated an outward current in HS-cells, which they concluded to be most likely a Na^{+}-dependent K^{+}-current, since it was abolished by the application of the Na^{+}-channel blocker tetrodotoxin. Activity-dependent adaptation in TCs might be regulated by this Na^{+}-dependent K^{+}-current, similar to spike-frequency adaptation in the visual cortex of ferrets (Sanchez-Vives et al., 2000a) and in the sensorimotor cortex of cats (Schwindt et al., 1989). Unfortunately, a potential role of Na^{+}-dependent K^{+}-currents in direction-selective adaptation of TCs is hard to test, because drug application interferes with the ability to elicit neuronal activity by sensory stimulation. Moreover,

methods to manipulate Na^+-concentrations in single neurons are, in contrast to Ca^{2+}, not yet established. Intracellular blockers of voltage-dependent Na^+ channels are available (QX-314), but are of limited value to clarify a potential role of Na^+ in TC adaptation, because Na^+ enters TC dendrites not only via voltage-dependent channels, but also through transmitter-gated channels at input synapses (Brotz and Borst, 1996).

Functional significance of direction-selective and direction-unselective adaptation

In contrast to studies of adaptation in many other neurons performing higher-order functions, it is possible in the *in vivo* preparation of the fly to directly evaluate the functional consequences of adaptation. Direction-selective and direction-unselective adaptation differ in their implications for the processing of sensory stimuli, because direction-selective processes are specifically associated only with those stimuli, which excite the neuron, whereas direction-unselective processes operate in a more general way. Direction-selective adaptation thus enables TCs to regulate their adaptational state by their own activity instead of by that in previous processing stages.

In the present study, I demonstrated that direction-selective adaptation in TCs is associated with a decrease in neuronal R_{in}. Carandini and Ferster (1997) could show that a tonic hyperpolarization underlies contrast adaptation in cat primary visual cortex, but sizable changes in R_{in} were not observed. In contrast, Sanchez-Vives et al. (2000b) demonstrated that decreases in neuronal R_{in} during post-adaptation hyperpolarization are present in at least a subgroup of neurons in cat primary visual cortex (see also for discussion: Carandini, 2000). With respect to the function of adaptation, it is highly relevant whether adaptation is associated with a change in R_{in} or not: adapting mechanisms causing a pure AHP without a change in R_{in} would lead to a pure subtractive shift of the input-response function of the neuron. In contrast, an AHP accompanied by a decrease in R_{in} as in fly TCs would cause both a subtractive shift and a divisive compression of the input-response relationship, i.e. a gain reduction.

The direction-selective component of adaptation might appear weak in comparison to the direction-unselective component. For three reasons however, direction-selective adaptation might nevertheless be highly significant for the system when operating under natural conditions. First, direction-selective adaptation builds up during the first few seconds after onset of strong motion stimulation whereas only later the influence of direction-unselective adaptation prevails (see Kurtz et al., 2000). The significance of components of adaptation, which build up fast may be underestimated relative to those that build up slowly when testing with constant motion stimuli instead of natural stimuli, which are shaped by the heterogeneous patterning of natural visual environments and frequent changes in flight direction. Second, direction-selective adaptation may lead to a change in directional tuning. In one scenario, the signals of several neurons, which are each tuned to different directions of motion, are integrated by a postsynaptic neuron. Direction-selective adaptation of individual input neurons would then dynamically modify the direction tuning of the integrating output neuron. Plasticity of neuronal tuning has already been demonstrated in the visual cortex of mammals (Dragoi et al., 2000), but not yet in the fly brain. Third, behavioral responses of the fly are often proposed to be regulated based on the comparison of neural responses between the two brain hemispheres. For example during rotational movements of the fly around its vertical body axis direction-unselective adaptation can be expected to be similar in both visual hemispheres. Direction-selective adaptation, in contrast, would differentially affect the neurons in the two brain hemispheres. Early observations of deviations in the resumption of a straight walking course after the cessation of rotatory visual motion, an after-effect similar to the well-known "waterfall illusion" in human perception, corroborate the notion that direction-selective adaptation has a significant impact on the behavioral level (Götz and Wenking, 1973; Srinivasan and Dvorak, 1979).

REFERENCES

Anderson JS, Carandini M, Ferster D (2000) Orientation tuning of input conductance, excitation, and inhibition in cat primary visual cortex. J Neurophysiol 84:909–926.

Benda J, Longtin A, Maler L (2005) Spike-frequency adaptation separates transient communication signals from background oscillations. J Neurosci 25:2312–2321.

Bhattacharjee A, Kaczmarek LK (2005) For K^+ channels, Na^+ is the new Ca^{2+}. Trends Neurosci 28:422–428.

Borst A, Egelhaaf M (1992) In vivo imaging of calcium accumulation in fly interneurons as elicited by visual motion stimulation. Proc Natl Acad Sci U S A 89:4139–4143.

Borst A, Flanagin VL, Sompolinsky H (2005) Adaptation without parameter change: Dynamic gain control in motion detection. Proc Natl Acad Sci U S A 102:6172–6176.

Borst A, Haag J (1996) The intrinsic electrophysiological characteristics of fly lobula plate tangential cells: I. Passive membrane properties. J Comput Neurosci 3:313–336.

Borst A, Haag J (2002) Neural networks in the cockpit of the fly. J Comp Physiol [A] 188:419–437.

Brenner N, Bialek W, de Ruyter van Stevenick RR (2000) Adaptive rescaling maximizes information transmission. Neuron 26:695–702.

Brotz TM, Borst A (1996) Cholinergic and GABAergic receptors on fly tangential cells and their role in visual motion detection. J Neurophysiol 76:1786–1799.

Carandini M (2000) Visual cortex: Fatigue and adaptation. Curr Biol 10:R605–R607.

Carandini M, Ferster D (1997) A tonic hyperpolarization underlying contrast adaptation in cat visual cortex. Science 276:949–952.

Chung S, Li X, Nelson SB (2002) Short-term depression at thalamo-cortical synapses contributes to rapid adaptation of cortical sensory responses in vivo. Neuron 34:437–446.

Clifford CW, Ibbotson MR (2002) Fundamental mechanisms of visual motion detection: models, cells and functions. Prog Neurobiol 68:409–437.

Crowder NA, Price NSC, Hietanen MA, Dreher B, Clifford CWG, Ibbotson MR (2006) Relationship between contrast adaptation and

orientation tuning in V1 and V2 of cat visual cortex. J Neurophysiol 95:271–283.

Dragoi V, Sharma J, Miller EK, Sur M (2002) Dynamics of neuronal sensitivity in visual cortex and local feature discrimination. Nat Neurosci 5:883–891.

Dragoi V, Sharma J, Sur M (2000) Adaptation-induced plasticity of orientation tuning in adult visual cortex. Neuron 28:287–298.

Dürr V, Egelhaaf M (1999) In vivo calcium accumulation in presynaptic and postsynaptic dendrites of visual interneurons. J Neurophysiol 82:3327–3338.

Eckert H (1981) The horizontal cells in the lobula plate of the blowfly, Phaenicia sericata. J Comp Physiol [A] 143:511–526.

Eckert H, Dvorak DR (1983) The centrifugal horizontal cells in the lobula plate of the blowfly, Phaenicia sericata. J Insect Physiol 29:547–560.

Egelhaaf M, Borst A (1989) Transient and steady-state response properties of movement detectors. J Opt Soc Am A 6:116–127.

Egelhaaf M, Borst A (1995) Calcium accumulation in visual interneurons of the fly: stimulus dependence and relationship to membrane potential. J Neurophysiol 73:2540–2552.

Egelhaaf M, Grewe J, Karmeier K, Kern R, Kurtz R, Warzecha AK (2005) Novel approaches to visual information processing in insects: case studies on neuronal computations in the blowfly. In: Methods in insect sensory neuroscience (Christensen TA, ed), pp 185–212. Boca Raton: CRC Press.

Egelhaaf M, Kern R, Krapp HG, Kretzberg J, Kurtz R, Warzecha A-K (2002) Neural encoding of behaviourally relevant visual-motion information in the fly. Trends Neurosci 25:96–102.

Fain GL, Matthews HR, Cornwall MC, Koutalos Y (2001) Adaptation in vertebrate photoreceptors. Physiol Rev 81:117–151.

Fettiplace R, Ricci AJ (2003) Adaptation in auditory hair cells. Curr Opin Neurobiol 13:446–451.

Götz KG, Wenking H (1973) Visual control of locomotion in walking fruitfly Drosophila. J Comp Physiol 85:235–266.

Gurney AM, Tsien RY, Lester HA (1987) Activation of a potassium current by rapid photochemically generated step increases of intracellular calcium in rat sympathetic neurons. Proc Natl Acad Sci U S A 84:3496–3500.

Haag J, Borst A (2002) Dendro-dendritic interactions between motion-sensitive large-field neurons in the fly. J Neurosci 22:3227–3233.

Haag J, Theunissen F, Borst A (1997) The intrinsic electrophysiological characteristics of fly lobula plate tangential cells: II. Active membrane properties. J Comput Neurosci 4:349–369.

Harris RA, O'Carroll DC, Laughlin SB (2000) Contrast gain reduction in fly motion adaptation. Neuron 28:595–606.

Hausen K (1982) Motion sensitive interneurons in the optomotor system of the fly: I. The horizontal cells: structure and signals. Biol Cybern 45:143–156.

Hengstenberg R (1977) Spike responses of 'non-spiking' visual interneurone. Nature 270:338–340.

Hengstenberg R (1982) Common visual response properties of giant vertical cells in the lobula plate of the blowfly Calliphora. J Comp Physiol [A] 149:179–193.

Huk AC, Rees D, Heeger DJ (2001) Neuronal basis of the motion aftereffect reconsidered. Neuron 32:161–172.

Ibbotson MR, Clifford CW, Mark RF (1998) Adaptation to visual motion in directional neurons of the nucleus of the optic tract. J Neurophysiol 79:1481–1493.

Kirschfeld K, Franceschini N (1977) Evidence for a sensitising pigment in fly photoreceptors. Nature 269:386–390.

Kohn A, Movshon JA (2004) Adaptation changes the direction tuning of macaque MT neurons. Nat Neurosci 7:764–772.

Krekelberg B, Boynton GM, van Wezel RJ (2006) Adaptation: from single cells to BOLD signals. Trends Neurosci 29:250–256.

Kurahashi T, Menini A (1997) Mechanism of odorant adaptation in the olfactory receptor cell. Nature 385:725–729.

Kurtz R (2004) Ca^{2+} clearance in visual motion-sensitive neurons of the fly studied in vivo by sensory stimulation and UV photolysis of caged Ca^{2+}. J Neurophysiol 92:458–467.

Kurtz R, Dürr V, Egelhaaf M (2000) Dendritic calcium accumulation associated with direction-selective adaptation in visual motion-sensitive neurons in vivo. J Neurophysiol 84:1914–1923.

Kurtz R, Warzecha AK, Egelhaaf M (2001) Transfer of visual motion information via graded synapses operates linearly in the natural activity range. J Neurosci 21:6957–6966.

Lancaster B, Nicoll RA, Perkel DJ (1991) Calcium activates two types of potassium channels in rat hippocampal neurons in culture. J Neurosci 11:23–30.

Lancaster B, Zucker RS (1994) Photolytic manipulation of Ca^{2+} and the time course of slow, Ca(2+)- activated K^+ current in rat hippocampal neurones. J Physiol 475:229–239.

Maddess T, Laughlin SB (1985) Adaptation of the motion-sensitive neuron H1 is generated locally and governed by contrast frequency. Proc R Soc Lond B Biol Sci 228:251–275.

Manookin MB, Demb JB (2006) Presynaptic mechanisms for slow contrast adaptation in mammalian retinal ganglion cells. Neuron 50:453–464.

Neri P, Laughlin SB (2005) Global versus local adaptation in fly motion-sensitive neurons. Proc Biol Sci 272:2243–2249.

Oertner TG, Brotz TM, Borst A (2001) Mechanisms of dendritic calcium signaling in fly neurons. J Neurophysiol 85:439–447.

Osmanovic SS, Shefner SA (1993) Calcium-activated hyperpolarizations in rat locus coeruleus neurons in vitro. J Physiol 469:89–109.

Sah P, Clements JD (1999) Photolytic manipulation of $[Ca^{2+}]i$ reveals slow kinetics of potassium channels underlying the afterhyperpolarization in hippocampal pyramidal neurons. J Neurosci 19:3657–3664.

Sanchez-Vives MV, Nowak LG, McCormick DA (2000a) Cellular mechanisms of long-lasting adaptation in visual cortical neurons in vitro. J Neurosci 20:4286–4299.

Sanchez-Vives MV, Nowak LG, McCormick DA (2000b) Membrane mechanisms underlying contrast adaptation in cat area 17 in vivo. J Neurosci 20:4267–4285.

Schwindt PC, Spain WJ, Crill WE (1989) Long-lasting reduction of excitability by a sodium-dependent potassium current in cat neocortical neurons. J Neurophysiol 61:233–244.

Schwindt PC, Spain WJ, Crill WE (1992) Effects of intracellular calcium chelation on voltage-dependent and calcium-dependent currents in cat neocortical neurons. Neuroscience 47:571–578.

Sengpiel F, Bonhoeffer T (2002) Orientation specificity of contrast adaptation in visual cortical pinwheel centres and iso-orientation domains. Eur J Neurosci 15:876–886.

Single S, Borst A (1998) Dendritic integration and its role in computing image velocity. Science 281:1848–1850.

Single S, Borst A (2002) Different mechanisms of calcium entry within different dendritic compartments. J Neurophysiol 87:1616–1624.

Single S, Haag J, Borst A (1997) Dendritic computation of direction selectivity and gain control in visual interneurons. J Neurosci 17:6023–6030.

Srinivasan MV, Dvorak DR (1979) The waterfall illusion in an insect visual system. Vision Res 19:1435–1437.

Tolias AS, Smirnakis SM, Augath MA, Trinath T, Logothetis NK (2001) Motion processing in the macaque: revisited with functional magnetic resonance imaging. J Neurosci 21:8594–8601.

Yazejian B, Sun XP, Grinnell AD (2000) Tracking presynaptic Ca^{2+} dynamics during neurotransmitter release with Ca^{2+}-activated K^+ channels. Nat Neurosci 3:566–571.